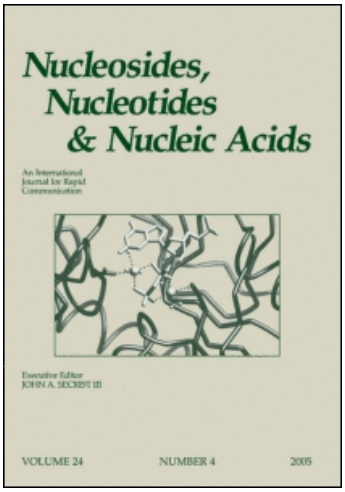

Nucleosides, Nucleotides and Nucleic Acids
Publication details, including instructions for authors and subscription information:
http://www.informaworld.com/smpp/title~content=t713597286

Hybridization of Antisense Oligonucleotides with α-Sarcin Loop Region of *Escherichia coli* 23S rRNA

Vladislav A. Petyuk[a]; Roman N. Serikov[a]; Valentin V. Vlassov[a]; Marina A. Zenkova[a]
[a] Institute of Chemical Biology and Fundamental Medicine, Novosibirsk, Russia

Online publication date: 10 July 2004

To cite this Article Petyuk, Vladislav A. , Serikov, Roman N. , Vlassov, Valentin V. and Zenkova, Marina A.(2004) 'Hybridization of Antisense Oligonucleotides with α-Sarcin Loop Region of *Escherichia coli* 23S rRNA', Nucleosides, Nucleotides and Nucleic Acids, 23: 6, 895 — 906
To link to this Article: DOI: 10.1081/NCN-200026038
URL: http://dx.doi.org/10.1081/NCN-200026038

NUCLEOSIDES, NUCLEOTIDES & NUCLEIC ACIDS
Vol. 23, Nos. 6 & 7, pp. 895–906, 2004

Hybridization of Antisense Oligonucleotides with α-Sarcin Loop Region of *Escherichia coli* 23S rRNA

Vladislav A. Petyuk, Roman N. Serikov, Valentin V. Vlassov, and Marina A. Zenkova*

Institute of Chemical Biology and Fundamental Medicine, Novosibirsk, Russia

ABSTRACT

Binding of complementary oligonucleotides (ONs) with α-sarcin loop region (2638–2682) of *Escherichia coli* 23S rRNA was investigated. Four of the tested pentadecanucleotides efficiently bound to target sequences with association rate and equilibrium constants $\sim 10^3$ $M^{-1}s^{-1}$ and 10^7 M^{-1}, respectively. ON S5 (CGAGAGGACCGGAGU) complementary to the sequence 2658–2672 displayed the highest affinity to the target. Activation energy for binding of ON S5 was measured to be 11 kcal/mol; this value corresponds to ~10% of the calculated enthalpy of the local RNA structure unfolding in the presence of this oligonucleotide. The activation energy value is evidence for the heteroduplex formation to occur via strand displacement pathway; the initiation of heteroduplex formation requires disruption of 1–2 base pairs in RNA hairpin.

Key Words: 23S rRNA alpha-sarcin loop; Antisense oligonucleotides; RNA structure; Strand displacement mechanism.

INTRODUCTION

Antisense technologies hold potential for gene therapy and study of gene functions.[1] One of the key problems in designing of efficient antisense oligonucleotides is

*Correspondence: Marina A. Zenkova, Institute of Chemical Biology and Fundamental Medicine, 8 Lavrentiev Ave., Novosibirsk, 630090, Russia; E-mail: marzen@niboch.nsc.ru.

DOI: 10.1081/NCN-200026038 1525-7770 (Print); 1532-2335 (Online)

identification of optimal sites for efficient oligonucleotide binding within target RNA.[2] Since RNAs are tightly folded and contain only short single-stranded regions, binding of oligonucleotides occurs through local unfolding of RNA structures and can cause global rearrangements of RNA structure. Apparently, efficacy of oligonucleotide binding is determined by stabilities of the elements of RNA structure involved in interaction, which are difficult to predict.[3] Earlier we demonstrated that heteroduplex formation could be initiated by interaction of oligonucleotides with short single-stranded sequences within the target site. An example is the hybridization of oligonucleotides to the 3′-part of yeast $tRNA^{Phe}$, which occurs through formation of a transient complex with a short single-stranded region at the CCA-end.[4,5]

Here we investigated the interaction of antisense oligonucleotides with α-sarcin loop region of 23S rRNA potential therapeutic target in ribosomes. We identified a pentadecamer CGAGAGGACCGGAGU that efficiently binds to the rRNA sequence 2658–2672 by strand displacement mechanism.

MATERIALS AND METHODS

Ribonucleotide triphosphates, deoxyribonucleotide triphosphates and dideoxyribonucleotide triphosphates were from Sigma. [γ-^{32}P]ATP and [α-^{32}P]ATP with specific activity of ~4000 Ci/mmol were from Biosan (Russia). Total tRNA from *Escherichia coli* used as a carrier to supplement labelled RNA, was from Vector (Russia). Ribonucleases T1, T2, CL3 and Deoxyribonuclease I (RNase free) were from Boehringer Mannheim (Germany). Ribonucleases ONE and V1 were from Promega (USA). T4 polynucleotide kinase was from SibEnzyme (Russia). AMV reverse transcriptase was from Life Science (USA). T7 RNA polymerase and Taq DNA polymerase were generous gifts of V. Ankilova and Dr. S. Khodyreva (this Institute), respectively. Oligodeoxyribonucleotides were synthesized by standard phosphoramidite chemistry and purified by ion-exchange and reverse-phase HPLC. 23S rRNA was isolated from *E. coli* 50S ribosomal subunits prepared according[6] using protocol described in Ref. [7].

Preparation of ECAS171 RNA

ECAS171 RNA was prepared by in vitro transcription using T7 RNA polymerase and template obtained by RT-PCR.[8] Oligonucleotides 5′-TAATACGACTCACTA-TAGGCGCTGGAGAACTGAGGG-3′ and 5′-GGGTCAGGGAGAACTCATCTCG-3′ were used as sense and antisense primers to amplify the 2625–2795 fragment of 23S rRNA of *Escherichia coli* and to insert a T7 promoter (T7 promotor sequence is underlined) at the 5′-end of PCR product for in vitro transcription.[9]

^{32}P Labelling of ECAS171 RNA

5′-end ^{32}P labelling of ECAS171 RNA was performed as described.[10] Prior to 5′-end labelling, ECAS171 in vitro transcript was dephosphorylated using bacterial alkaline phosphatase. Labelling of the transcript was performed with [γ-^{32}P]ATP and T4 polynucleotide kinase under standard conditions. Uniformly labelled ECAS171 RNA was prepared by in vitro transcription using [α-^{32}P]ATP and T7 RNA polymerase

as described in Ref. [10]. Secondary structure of the ECAS171 RNA was confirmed using probing with ribonucleases T1, T2, CL3, ONE and V1 as described in.[11]

Hybridization of Oligonucleotides with ECAS171 RNA

Hybridization of oligonucleotides with ECAS171 RNA was analyzed using gel-mobility shift assay.[12] Reaction mixtures (10 μl) containing 50 mM Cacodylate-HCl pH 7.3, 0.1 mM EDTA (300 mM KCl and 10 mM $MgCl_2$ optionally), 10 nM (0.1 μCi) uniformly-labelled ECAS171 RNA were consecutively incubated at 75°C for 1 min, at 37°C for 15 min and at temperatures from 0 to 37°C (see figure legends) for 15 min. Then oligonucleotide was added at concentration ranging from 0.01 μM to 10 μM and probes were incubated at hybridization temperatures for 1–2 h. After incubation, 3 μl of loading buffer (20% Ficoll-400, 0.025% bromphenol blue, 0.025% xylen cyanol) was added to each reaction and the mixtures were analyzed by electrophoresis in native 6% PAGE at 20 V/cm, at 4°C. Free RNA was separated well from the oligonucleotide bound one. Excision of radioactive bands from the polyacrylamide gel followed by Cerenkov counting of the bands allowed quantitation of free and oligonucleotide bound ECAS171 RNA.

Hybridization kinetics were analyzed similarly except for 60 μl reaction mixtures were used. After the renaturation, oligonucleotides were added to the reaction mixtures at a final concentration 1 μM. Aliquots (5 μl) were taken from the reaction mixture, mixed with loading buffer (1.5 μl), and applied on running (20 V/cm) native 6% PAGE.

Equilibrium association constants (K_a) were calculated by minimizing mean square deviation between experimental curves and calculated ones, obtained with the equation: $a = \frac{K_a \cdot [ON]}{1 + K_a \cdot [ON]}$, where K_a is equilibrium association constant, a-binding extent, *[ON]*-oligonucleotide concentration.

The direct and reverse rate constants were calculated by minimizing mean square deviation between experimental curves and calculated ones, using the equation: $a = \frac{k_+ \cdot [ON]}{k_+ \cdot [ON] + k_-} \cdot (1 - e^{-t \cdot (k_+ \cdot [ON] + k_-)})$, where a is binding extent, k_+ and k_- direct and reverse rate constant, respectively, *[ON]*-oligonucleotide concentration. All mean square calculations were performed using Origin 7.0 software.

RESULTS

RNA and Oligonucleotides Design

The α-sarcin domain of 23S rRNA contains a loop with the longest universally conserved sequence present in large ribosomal RNAs.[13] The integrity of the α-sarcin loop is essential for ribosome function: hydrolysis of one phosphodiester bond after G2661 by highly specific RNase α-sarcin or depurination of A2660 by ricin blocks elongation.[14] The structure of this site in 23S rRNA has been investigated in detail by chemical and enzymatic probing,[15] NMR spectroscopy[16] and X-ray crystallography.[17] The α-sarcin loop was found to fold in a highly compact structure forming GAGA tetraloop, which belongs to extremely stable GNRA tetraloop family.[18–20]

We have chosen domain VIA of 23S rRNA containing helixes 94–97 as a target for antisense oligonucleotides.[21] 171-nucleotides long RNA fragment was designed using a computer search so as to retain native structure and have terminus convenient

for labelling. Hereafter this RNA fragment is named ECAS171 (*Escherichia coli* α-sarcin 171-nucleotides long). The secondary structure of ECAS171 RNA was investigated by enzymatic probing using RNases T1, T2, CL3, ONE and V1. The reactivities of nucleotides and the derived secondary structure of ECAS171 RNA are in a good agreement with previously published data on chemical and enzymatic probing of 23S rRNA *E. coli*.[15]

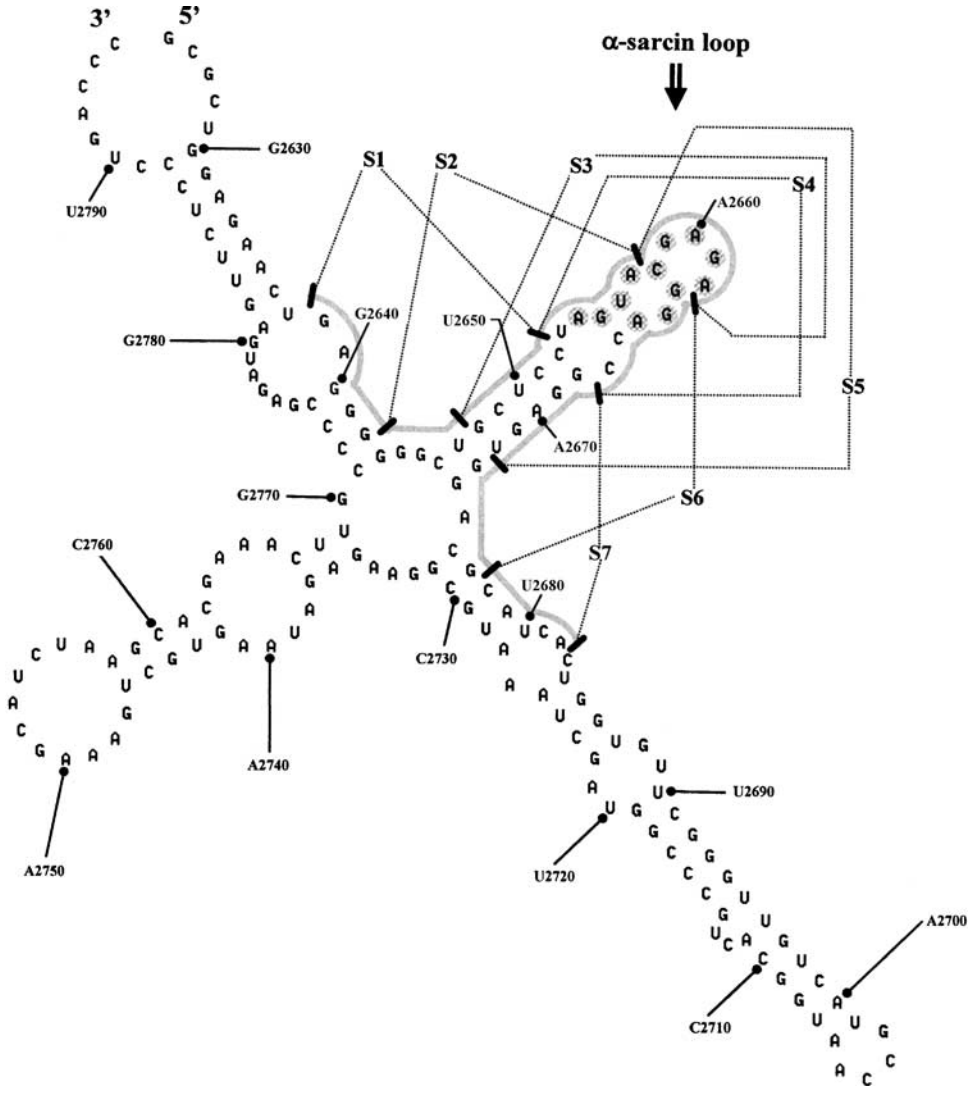

Figure 1. Secondary structure of the ECAS171 RNA fragment of 23S rRNA *Escherichia coli* and complementary sites for oligonucleotides S1–S7. Grey line indicates the target region for the oligonucleotides. Marks show division of the target region into 5-nucleotide fragments. Complementary sites for each oligonucleotide consisting of 3 neighboring 5-nucleotide fragments are marked by dotted lines. 12 conserved nucleotides of the α-sarcin loop are indicated by gray circles.

The target sites for seven pentadecamers S1–S7 located within 45-nt region of ECAS171 RNA (corresponds to sequence 2638–2682 of 23S rRNA) containing α-sarcin loop are shown in Fig. 1. The target sites are arranged symmetrically relative to the α-sarcin loop: the sites for oligonucleotides S1, S2, S3 are symmetrical to those for oligonucleotides S7, S6, S5, respectively. Oligonucleotide S4 is complementary to the entire α-sarcin loop. These sites represent a 5-nucleotide step shifting, i.e. any site can be obtained by shifting the previous one by 5 nucleotides.

Hybridization of Oligonucleotides S1–S7 with ECAS171 RNA

Hybridization of oligonucleotides with ECAS171 RNA was investigated under physiological conditions (pH 7.5, 350 mM of monovalent cations, 10 mM $MgCl_2$, 37°C) using gel-mobility shift assay (Fig. 2). Hybridization was performed at a constant concentration of [^{32}P]-uniformly labelled ECAS171 RNA and various concentrations of oligonucleotides S1–S7. Free RNA was electrophoretically separated from the complex. Excision of radioactive bands from the polyacrylamide gel followed by Cherenkov counting of the bands allowed quantification of free and oligonucleotide bound ECAS171 RNA. No hybridization was observed for ONs S1 and S2 (Fig. 2) that were complementary to the 5′ part of the target region. ON S3 displayed poor hybridization efficiency. ONs S4–S7 complementary to the loop region and 3′ part of the α-sarcin hairpin bound to the RNA with high efficiency. Oligonucleotides S6 and S7 complementary to the 3′ part of the target region yielded complexes with abnormally low electrophoretic mobilities.

Annealing of ONs with ECAS171 RNA yielded the same levels of binding as achieved after one hour incubation at 37°C. Similar hybridization yields were observed in solutions containing 10 mM Mg^{2+} and in solutions free of magnesium ions. This fact

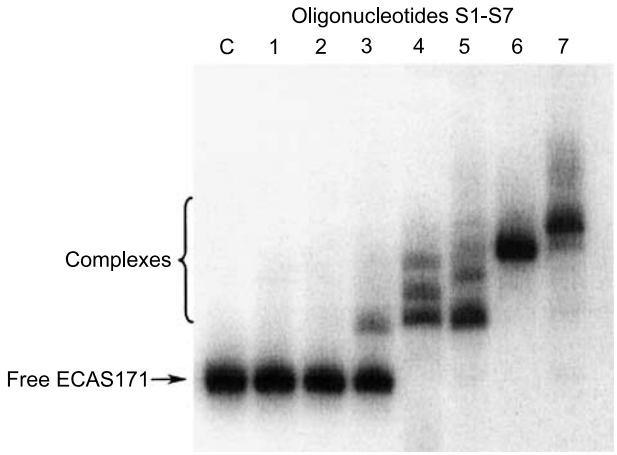

Figure 2. Gel-shift analysis of oligonucleotides S1–S7 hybridization with ECAS171 RNA. Autoradiogram of 6% native polyacrylamide gel showing free and oligonucleotide bound ECAS171 RNA. ^{32}P-ECAS171 (0.01 μM) was incubated with oligonucleotides (10 μM) for 1 hour at 37°C in 50 mM Cacodylate-HCl pH 7.3, containing 300 mM KCl and 0.1 mM EDTA.

Table 1. Equilibrium constants of oligonucleotides binding to ECAS171 RNA at 37°C in 50 mM cacodylate-HCl buffer pH 7.3, containing 300 mM KCl and 0.1 mM EDTA.

Oligonucleotide	K_x (M^{-1})
S1	–
S2	–
S3	$\leq 3 \cdot 10^4$
S4	$(2.8 \pm 0.3) \cdot 10^7$
S5	$(4.3 \pm 0.6) \cdot 10^7$
S6	$(2.5 \pm 0.3) \cdot 10^6$
S7	$(6.6 \pm 1.0) \cdot 10^5$

is in accordance with data obtained by X-ray crystallography[17] indicating that α-sarcin domain contains no binding sites for bivalent cations.

The equilibrium binding constants determined for oligonucleotides S3–S7 are listed in Table 1. ONs S1, S2 and S3 display absence or poor affinity to the RNA. The group with oligonucleotides S6 and S7 demonstrate moderate affinity and ONs S4 and S5 form tight complexes.

The influence of magnesium on equilibrium and association rate constants was investigated in experiments with ON S5 (Tables 2 and 3). In the presence of 10 mM magnesium chloride both equilibrium constant and association rate constant are slightly decreased: from $(4.3 \pm 0.6) \cdot 10^7$ to $(2.5 \pm 0.5) \cdot 10^7$ M^{-1} and from $(1.8 \pm 0.1) \cdot 10^3$ to $(1.2 \pm 0.1) \cdot 10^3$ $M^{-1}s^{-1}$, respectively. This can be explained by stabilization of the rRNA structure by increase of salt concentration. This effect is much less pronounced as compared to the influence of Mg^{2+} ions on oligonucleotide hybridization with yeast $tRNA^{Phe}$, containing strong Mg^{2+} binding sites.[22] In this latter case more than 10 fold decrease of association constant of oligonucleotides occurred in the presence of 5 mM $MgCl_2$. Magnesium ions strongly decrease the efficiency of oligonucleotide hybridization to RNA structures containing sites for tight binding of divalent cations: tRNAs,[5] HIV-1 genomic RNA, and ribozymes.[23] It seems that magnesium ions will not be a significant obstacle for oligonucleotide hybridization with rRNAs and mRNAs.

Table 2. Rate constants of oligonucleotide S5 hybridization to ECAS171 RNA: effect of temperature and Mg^{2+} ions.

Temperature, °C	k_+ ($M^{-1}s^{-1}$)
0.0	$(4.9 \pm 0.5) \cdot 10^2$
9.1	$(8.0 \pm 0.4) \cdot 10^2$
15.0	$(1.2 \pm 0.1) \cdot 10^3$
20.0	$(1.8 \pm 0.1) \cdot 10^3$
25.0	$(2.8 \pm 0.2) \cdot 10^3$
20.0 (+ Mg)*	$(1.2 \pm 0.1) \cdot 10^3$

*In the presence of 5 mM $MgCl_2$.

Table 3. Temperature dependence of equilibrium binding constant for oligonucleotide S5.

Temperature (°C)	K_x (M^{-1})
37	$(4.3 \pm 0.6)\cdot 10^7$
25.1	$(2.3 \pm 0.4)\cdot 10^7$
20.1	$(1.6 \pm 0.4)\cdot 10^7$
16.3	$(1.4 \pm 0.4)\cdot 10^7$
12.6	$(1.2 \pm 0.3)\cdot 10^7$
8.2	$(8.9 \pm 2.2)\cdot 10^6$
0	$(5.6 \pm 1.3)\cdot 10^6$

Kinetics of Oligonucleotide S5 Hybridization with ECAS171 RNA. Calculation of Hybridization Activation Energy (E_a)

We compared the experimental values of enthalpy and activation energy in order to find out whether hybridization occurs via dissociative or strand displacement pathways.[24] Hybridization kinetics were investigated within the temperature interval ranging from 0 to 25°C, because at 37°C ON S5 hybridized with the RNA too fast to

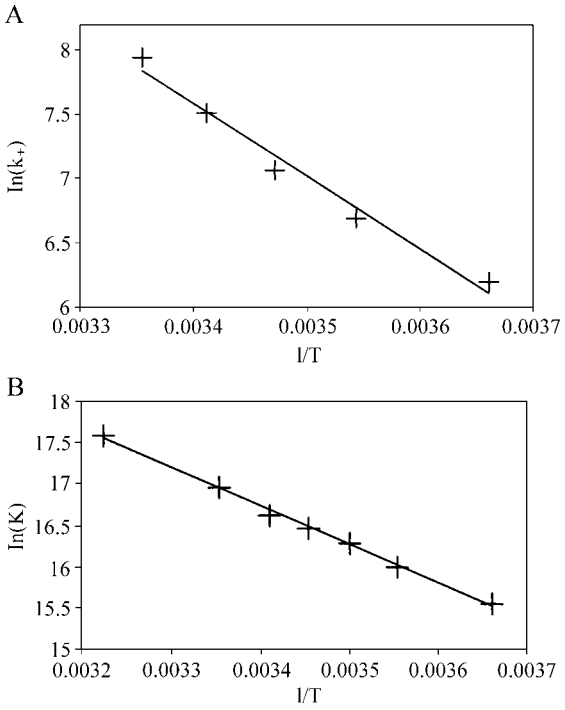

Figure 3. Activation energy and enthalpy of ON S5 hybridization with ECAS171 RNA. A) Arrhenius plot ($\ln(k_+)$ vs 1/T) of hybridization rate constants (Table 2) for oligonucleotide S5. B) Equilibrium binding constants (Table 3) plotted into ln(K) vs 1/T coordinates.

obtain adequate quantitative data using gel mobility-shift assay. At 20°C the plateau binding level was achieved after 1 hour of incubation (data not shown).

For analysis of kinetic curves we used a quasilinear approximation of bimolecular reversible reaction. The apparent hybridization rate constants for ON S5 were measured at different temperatures and buffer conditions. An Arrhenius plot of the dependence of hybridization rate constant versus temperature ($\ln(k_+)$ versus 1/T) is shown in Fig. 3 and listed in Table 2. The linearity of the curve within the temperature interval between 0°C and 25°C is in agreement with the assumption that the mechanism of the complex formation does not change within this temperature interval. The dependence of k_+ on temperature was used to estimate the activation energy (E_a) of the hybridization reaction according to the Arrhenius equation ($\ln(k_+) = -E_a/kT + \ln(A)$, A = const.). The association rate increases with increasing of the temperature, indicating that the activation energy is positive, which is not always the case, for example, for short oligonucleotides.[25] The activation energy of the complex formation of oligonucleotide S5 and ECAS171, was determined to be $E_a = 11 \pm 1$ kcal/mol.

In order to determine enthalpy and entropy of oligonucleotide S5 binding with ECAS171 RNA, we measured temperature dependence of the equilibrium association constant (Fig. 3 and Table 3) in the same temperature interval (from 0°C to 25.1°C). The values of enthalpy and entropy of hybridization were determined according to the equation $\ln(K_a) = -\Delta H/RT + \Delta S/R$. Enthalpy was found to be $\Delta H = -9.0 \pm 0.2$ kcal/mol, and entropy $\Delta S = 63.8 \pm 0.8$ cal/mol·K.

DISCUSSION

Oligonucleotides S1–S7 displayed considerably different affinities to ECAS171 RNA. Apparently, such significant differences reflect both stability of the formed heteroduplexes and stability of RNA structures to be unfolded at the oligonucleotide binding sites. We used hybridization conditions (37°C, 350 mM monovalent cations) suitable for comparison of experimentally determined ΔG values with those calculated using different algorithms and computer programs.[3,26,27] Magnesium ions were omitted because they can be coordinated as inner-sphere ligands significantly stabilising RNA structure, which is difficult to predict. Moreover, ''nearest-neighbour'' parameters for calculation of DNA/RNA heteroduplex stability were obtained in the absence of magnesium ions. In general, the calculated ΔG values are lower than those ones determined from experiments (Fig. 4): the differences vary from 0.8 kcal/mol for S7 up to 8.3 kcal/mol for S4. Predicted affinities for oligonucleotides S1 and S4 appeared to be significantly overestimated as compared to the data for other oligonucleotides. In contrast, for the ON S7, the calculated ΔG value is lower then the measured one. Moreover, calculations according to algorithms predict, that ON S4 should be the most efficient in binding to ECAS171 RNA. However, the experimental data shows that ON S5 binds to the RNA better then S4. This fact can be ascribed to the properties of the the α-sarcin loop structure. The affinity of oligonucleotide S1 to the RNA is very low as compared to the theoretical predictions. Complementary site for oligonucleotide S1 contains a track of six guanosines (4 GC pairs and 2 unpaired G), which might form a local non-canonical structure. There is a possibility that the guanines are stacked additionally stabilising the local RNA structure. This is in

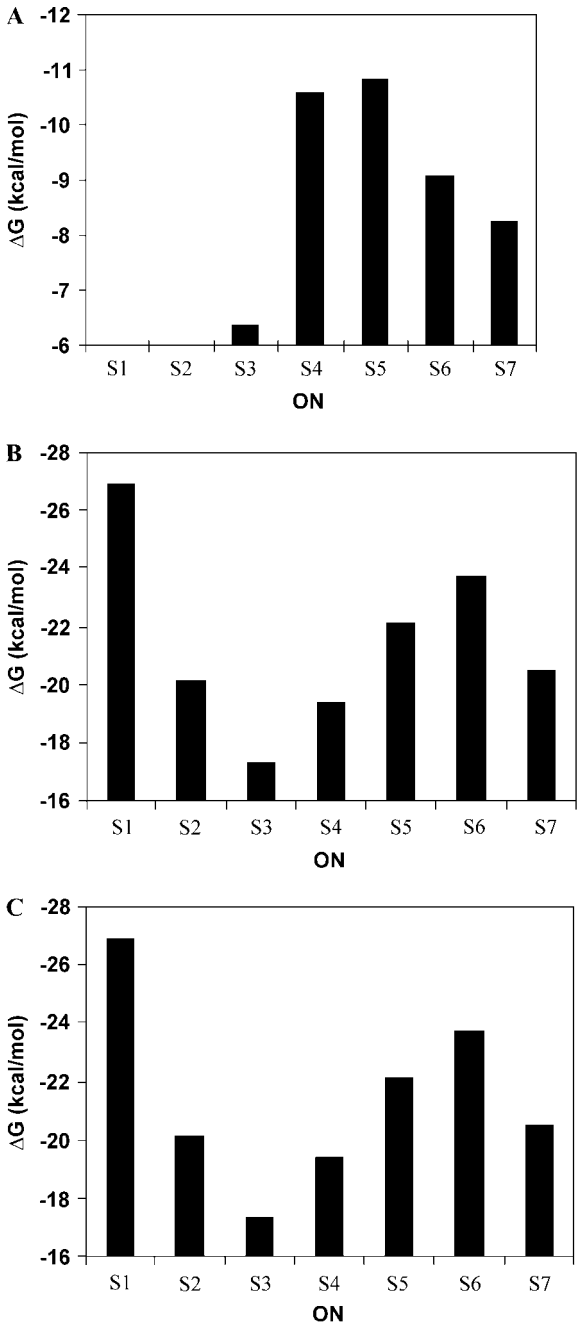

Figure 4. Stabilities of heteroduplexes (ΔG) formed by oligonucleotides S1–S5 and ECAS171 RNA at 37°C. (A) Experimentally determined ΔG values. (B) ΔG values calculated using ''nearest neighbor'' approach for 37°C: heteroduplexes are formed with 15-mer linear RNA complementary strands. (C) ΔG values for oligonucleotides hybridization with ECAS171 RNA at 37°C, calculated taking into account ΔG of RNA refolding after oligonucleotide binding.

agreement with RNase V1 probing (data not shown): G2645 expected to be in a single-stranded region is cleaved by RNase V1. In particular, it is quite possible, that G-A pair formed between G2639 and A2775[28,29] closes the stem of 4 GC pairs.

Recently we have shown that oligonucleotide hybridization with yeast $tRNA^{Phe}$ occurs as a two-step process, including fast formation of an intermediate complex with the open single stranded regions of the RNA followed by the rate limiting intramolecular rearrangement of intermediate complex into stable full-length complex.[5] According to our data, the limiting step of oligonucleotide hybridization with RNA is unfolding of the RNA local structure at the binding site.

Heteroduplex formation can occur through two pathways.[24] The first one is a dissociation-like process, which consists in unfolding of RNA at the target site followed by oligonucleotide binding to the formed single-stranded region. The second one is a mechanism similar to the ''strand displacement'' process-stepwise invasion of the oligonucleotide displacing elements of the RNA structure that interacts with its complement. In the first case the value of activation energy (E_a) is expected to be close to an enthalpy of the RNA structure unfolding at the target site. In the second case the E_a value should be significantly lower and corresponds to the ΔH value of opening of several base pairs at the target region needed for the displacement initiation. The enthalpy of RNA structure unfolding can be estimated from experimentally determined enthalpy of oligonucleotide hybridization ($\Delta H_{binding}$ = 9.0 kcal/mol) and theoretically calculated enthalpy of heteroduplex (ΔH_{heter} = − 128.6 kcal/mol). For the case of oligonucleotide S5: $\Delta H_{unfold} = \Delta H_{binding} - \Delta H_{heter}$, ΔH_{unfold} = 137.6 kcal/mol. The apparent activation energy measured for oligonucleotide S5 is E_A = 11 kcal/mol. Thus, in the case of oligonucleotide S5, E_a value corresponds to ~8% of enthalpy of the local RNA structure unfolding. These data show that interaction of ON S5 with ECAS171 RNA occurs through a process similar to strand-displacement. The similar value of activation energy E_a = 10.2 kcal/mol was reported earlier for hybridization of sense and antisense RNA fragments.[30]

The values of E_a (11 and 10.2 kcal/mol) are close to the enthalpy of disruption of 1 or 2 Watson-Crick base pairs. ΔH values for GC and AU base pairs are: 13–14 kcal/mol and 6–8 kcal/mol, respectively.[31] The strand-displacement mechanism operated in the process of replacement of a DNA oligonucleotide probe bound to a complementary DNA target with an another probe of the same sequence. The contribution of the displacement pathway is predominant over the dissociative pathway at temperatures lower then melting temperatures of the target duplexes. This is the case for oligonucleotide S5 hybridization with ECAS171 RNA at 0–25°C. In the case of DNA, strand displacement is isoenergetic. Invasion of oligonucleotides into RNA structure can require some energy because of higher stabilities of RNA/RNA duplex then of DNA/RNA ones. Moreover, tertiary structure of RNA can provide additional obstacles in heteroduplex elongation.

Results of the present study demonstrate that currently available theoretical approaches cannot always accurately predict oligonucleotide affinities to RNA targets because the target sequences can be involved in tertiary interactions, and stabilities of local specific structures cannot be easily predicted. We have identified oligonucleotide S5 complementary to the sequence 2658–2672 that is capable of tight binding to α-sarcin loop region of 23S rRNA. This oligonucleotide can be considered as a prototype of an antibacterial oligonucleotide-based therapeutic targeted to ribosomal RNA.

ACKNOWLEDGMENTS

This work was supported by INTAS (96-1418), RFBR (02-04-48559 and SS-1384.2003.4), CRDF (REC-008), SB RAS (Interdisciplinary grant and Young Scientist grant). We thank Dr. Elena Kostenko for technical help in preparation of ECAS171 RNA.

REFERENCES

1. Crooke, S.T. Potential roles of antisense technology in cancer chemotherapy. Oncogene **2000**, *19*, 6651–6659.
2. Branch, A.D. A good antisense molecule is hard to find. Trends Biochem. Sci. **1998**, *23*, 45–50.
3. Walton, S.P.; Stephanopoulos, G.N.; Yarmush, M.L.; Roth, C.M. Prediction of antisense oligonucleotide binding affinity to a structured RNA target. Biotechnol. Bioeng. **1999**, *65*, 1–9.
4. Petyuk, V.; Zenkova, M.; Giege, R.; Vlassov, V. Interaction of complementary oligonucleotides with the 3′-end of yeast $tRNA^{Phe}$. Nucleosides Nucleotides Nucl. Acids **1999**, *18*, 1459–1461.
5. Petyuk, V.A.; Giege, R.; Vlassov, V.V.; Zenkova, M.A. Mechanism of oligonucleotide interaction with the 3′ part of yeast $tRNA^{Phe}$. Mol. Biol. (Moscow) **2000**, *34*, 886–889.
6. Makhno, V.I.; Peshin, N.N.; Semenkov, I.P.; Kirillov, S.V. A modified method of isolation of ''tight'' 70S ribosomes from *Escherichia coli* highly active at different stages of the elongation cycle. Mol. Biol. (Moscow) **1988**, *22*, 670–679.
7. Abdukaiumov, M.; Gimautdinova, O.I.; Graifer, D.M.; Zenkova, M.A.; Karpova, G.G. Preparation of *Escherichia coli* 70S ribosomes labelled with 35S. (Article in Russian). Biokhimiia **1987**, *52*, 1411–1416.
8. Walker, S.C.; Avis, J.M.; Conn, G.L. General plasmids for producing RNA in vitro transcripts with homogeneous ends. Nucleic Acids Res. **2003**, *31*, 82.
9. Sambrook, J.; Fritsch, E.M.; Maniatis, T. *Molecular Cloning: A Laboratory Manual*, 2nd Ed.; Cold Spring Harbor: New York, 1989; pp. 14.16–14.20, 8.11–8.13.
10. Silberklang, M.; Prochiantz, A.; Haenni, A.L.; Rajbhandary, U.L. Studies on the sequence of the 3′-terminal region of turnip-yellow-mosaic-virus RNA. Eur. J. Biochem. **1977**, *72*, 465–478.
11. Ehresmann, C.; Baudin, F.; Mougel, M.; Romby, P.; Ebel, J.P.; Ehresmann, B. Probing the structure of RNAs in solution. Nucleic Acids Res. **1987**, *15*, 9109–9128.
12. Ceglarek, J.A.; Revzin, A. Studies of DNA-protein interactions by gel electrophoresis. Electrophoresis **1989**, *10*, 360–365.
13. Wool, I.G., Endo, Y., Chan, Y.-L., Gluck, A. In *The Ribosome: Structure, Function and Evolution*; Hill, W.E., Dahlberg, A., Garret, R.A., Moore, P.B., Schlessinger, D., Warner, J.R., Eds.; American Society for Microbiology, Washington, D.C., 1990; 203–214.
14. Endo, Y.; Wool, I.G. The site of action of alpha-sarcin on eukaryotic ribosomes. The sequence at the alpha-sarcin cleavage site in 28 S ribosomal ribonucleic acid. J. Biol. Chem. **1982**, *257*, 9054–9060.

15. Leffers, H.; Egebjerg, J.; Andersen, A.; Christensen, T.; Garrett, R.A. Domain VI of Escherichia coli 23S ribosomal RNA. Structure, assembly and function. J. Mol. Biol. **1988**, *204*, 507–522.
16. Szewczak, A.A.; Moore, P.B.; Chan, Y.; Wool, I.G. The conformation of the sarcin/ricin loop from 28S ribosomal RNA. Proc. Natl. Acad. Sci. U. S. A. **1993**, *90*, 9581–9585.
17. Correll, C.C.; Wool, I.G.; Munishkin, A. The two faces of the *Escherichia coli* 23S rRNA sarcin/ricin domain: the structure at 1.11 A resolution. J. Mol. Biol. **1999**, *292*, 275–287.
18. Brion, P.; Westhof, E. Hierarchy and dynamics of RNA folding. Annu. Rev. Biophys. Biomol. Struct. **1997**, *26*, 113–137.
19. Strobel, S.A.; Doudna, J.A. RNA seeing double: close-packing of helices in RNA tertiary structure. Trends Biochem. Sci. **1997**, *22*, 262–266.
20. Jagath, J.R.; Matassova, N.B.; de Leeuw, E.; Warnecke, J.M.; Lentzen, G.; Rodnina, M.V.; Luirink, J.; Wintermeyer, W. Important role of the tetraloop region of 4.5S RNA in SRP binding to its receptor FtsY. RNA **2001**, *7*, 293–301.
21. Lieberman, K.R.; Firpo, M.A.; Herr, A.J.; Nguyenle, T.; Atkins, J.F.; Gesteland, R.F.; Noller, H.F. The 23 S rRNA environment of ribosomal protein L9 in the 50 S ribosomal subunit. J. Mol. Biol. **2000**, *297*, 1129–1143.
22. Misra, V.K.; Draper, D.E. The linkage between magnesium binding and RNA folding. J. Mol. Biol. **2002**, *317*, 507–521.
23. Hammann, C.; Norman, D.G.; Lilley, D.M. Dissection of the ion-induced folding of the hammerhead ribozyme using 19F NMR. Proc. Natl. Acad. Sci. U. S. A. **2001**, *98*, 5503–5508.
24. Reynaldo, L.P.; Vologodskii, A.V.; Neri, B.P.; Lyamichev, V.I. The kinetics of oligonucleotide replacements. J. Mol. Biol. **2000**, *297*, 511–520.
25. Porschke, D.; Eigen, M. Co-operative non-enzymic base recognition. 3. Kinetics of the helix-coil transition of the oligoribouridylic–oligoriboadenylic acid system and of oligoriboadenylic acid alone at acidic pH. J. Mol. Biol. **1971**, *62*, 361–381.
26. Sugimoto, N.; Nakano, S.; Katoh, M.; Matsumura, A.; Nakamuta, H.; Ohmichi, T.; Yoneyama, M.; Sasaki, M. Thermodynamic parameters to predict stability of RNA/DNA hybrid duplexes. Biochemistry **1995**, *34*, 11211–11216.
27. Mathews, D.H.; Burkard, M.E.; Freier, S.M.; Wyatt, J.R.; Turner, D.H. Predicting oligonucleotide affinity to nucleic acid targets. RNA **1999**, *5*, 1458–1469.
28. Traub, W.; Sussman, J.L. Adenine-guanine base pairing ribosomal RNA. Nucleic Acids Res. **1982**, *10*, 2701–2708.
29. SantaLucia, J.; Kierzek, R.; Turner, D.H. Effects of GA mismatches on the structure and thermodynamics of RNA internal loops. Biochemistry **1990**, *29*, 8813–8819.
30. Homann, M.; Rittner, K.; Sczakiel, G. Complementary large loops determine the rate of RNA duplex formation in vitro in the case of an effective antisense RNA directed against the human immunodeficiency virus type 1. J. Mol. Biol. **1993**, *233*, 7–15.
31. Borer, P.N.; Dengler, B.; Tinoco, I., Jr.; Uhlenbeck, O.C. Stability of ribonucleic acid double-stranded helices. J. Mol. Biol. **1974**, *86*, 843–853.

Received December 2, 2003
Accepted April 23, 2004